Article

Parametric Analysis of a Solar Water Heater Integrated with PCM for Load Shifting

Sofiene Mellouli [1],*, Talal Alqahtani [2] and Salem Algarni [2]

1. College of Engineering, Mechanical Engineering Department, Jazan University, Jazan 45142, Saudi Arabia
2. College of Engineering, Mechanical Engineering Department, King Khalid University, Abha 61421, Saudi Arabia
* Correspondence: sofiene.mellouli81@gmail.com

Abstract: Integrating a solar water heater (SWH) with a phase change material (PCM)-based latent heat storage is an attractive method for transferring load from peak to off-peak hours. This transferring load varies as the physical parameters of the PCM change. Thus, the aim of this study is to perform a parametric analysis of the SWH on the basis of the PCM's thermophysical properties. A mathematical model was established, and a computation code was developed to describe the physical phenomenon of heat storage/release in/from the SWH system. The thermal energy stored and the energy efficiency are used as key performance indicators of the new SWH–PCM system. The obtained numerical results demonstrate that the used key performance indicators were significantly impacted by the PCM thermo-physical properties (melting temperature, density, and latent heat). Using this model, various numerical simulations are performed, and the results indicate that, SWH with PCM, 20.2% of thermal energy on-peak periods load is shifted to the off-peak period. In addition, by increasing the PCM's density and enthalpy, higher load shifting is observed. In addition, the PCM, which has a lower melting point, can help the SWH retain water temperature for a longer period of time. There are optimal PCM thermo-physical properties that give the best specific energy recovery and thermal efficiency of the SWH–PCM system. For the proposed SWH–PCM system, the optimal PCM thermo-physical properties, i.e., the melting temperature is 313 K, the density is 3200 kg/m^3, and the latent heat is 520 kg/kg.

Keywords: solar water heater; latent heat storage; PCM; load shifting

1. Introduction

The current energy context is characterized by the depletion of fossil fuel resources on the one hand and global warming as a result of greenhouse gas emissions on the other, necessitating the development of alternative energy solutions. Among the alternatives being investigated is the effective utilization of renewable energy sources. Energy use in buildings, namely for air cooling and water heating, accounts for around two-thirds of total energy demands. Consequently, it is imperative to limit building energy use. Shifting a part of peak-period electricity usage to off-peak periods could have substantial economic, environmental, and social consequences. Solar energy has the greatest potential of all renewable energies [1]. This kind of energy poses storage issues, as thermal energy can be stored as either sensible or latent heat. Storing surplus solar thermal energy and utilizing it during the night period would improve the operation and effectiveness of solar water heaters. Integrating thermal energy storage through latent heat thermal energy is a promising method for off-peak load shifting. Thermal energy storage systems can be used in conjunction with building walls, solar water collectors, and domestic hot water tanks. Domestic hot water production is receiving more attention at the moment due to concerns about its energy efficiency, as well as the size and number of storage tanks. The incorporation of phase change materials (PCM) enables the provision of solutions by

storing thermal energy via latent heat rather than sensible heat, as indicated by the extensive literature in the domain [1–3]. The research conducted focuses primarily on the precise investigation of heat transfer within various types of water heaters using computational [4] and/or experimental [5] methodologies. The following are the most frequently used designs for solar water heaters with latent heat storage: (i) the use of PCM capsules in a water tank powered by standard solar collectors, (ii) the combination of a standard solar collector and a separate PCM unit, and (iii) the use of integrated solar collectors and PCM [2]. Solar thermal storage combined with a latent storage system based on PCMs is an intriguing solution for more efficient energy use. As a result, numerous studies have been conducted on the study and modeling of solar collectors [3–7]. Sharma et al. [3] summarized existing research on this topic by evaluating PCM-based storage devices and their applications in solar, building insulation, and aerospace. Additionally, they demonstrated techniques for measuring latent heat and temperature. Comparative studies on the usage of various types of storage in conjunction with PCM have been conducted. Kurklu et al. [4] designed a novel type of solar collector in which a water tank is integrated with a PCM unit with a melting point of 45 to 50 °C. The results indicated that the reservoir temperature is maintained at 30 °C throughout the night on a sunny day. Additionally, the immediate thermal efficiency ranged from roughly 22% to 80%. Zalba [5] investigates several PCM kinds. It lists approximately 150 materials that have been used and 45 that have been commercialized; therefore, there is a vast array of PCM materials available. The advantages of PCM systems are discussed, including the high-equivalent specific heat produced by phase change and the ability to regulate the water temperature. Nonetheless, important issues, such as stability, lifespan, storage capacity reduction based on the number of working cycles, and hazardous dangers in the event of a fire are noted. Eames and Griffiths [6] investigated the collector and heat storage in a self-storing collector when water was replaced with PCM in various quantities. They noted that as long as the temperature inside the tank remains below the melting point (58–60 °C), the efficiency of the solar system with PCM is lower than that of a system filled entirely with water. Plantier et al. [7] conducted research on a water tank filled with PCM spheres. It demonstrates that the use of PCM increases storage density and enables temperature control within the tank. The low thermal conductivity of PCM was mentioned as one of the issues. Additionally, the spheres were too massive to be extracted efficiently. To remedy this problem, Haillot et al. [8] numerically and experimentally addressed the challenge of a solar collector incorporating a PCM/graphite mixture as a storage medium. This system enables greater storage and extraction of solar energy due to its storage capacity and the high thermal conductivity of graphite. During withdrawal, the efficiency of the solar collector integrating the storage is around 98%, demonstrating the high discharge capacity of the system. Other advantages are noted, such as the reduction in the stagnation temperature and storage volume. Mettaweea et al. [9] conducted an experiment to evaluate the performance of a compact solar–PCM collector system. The results demonstrated that the average heat transfer coefficient increases with increasing thickness of the paraffin layer, owing to natural convection. The problems of solid–liquid phase change are of remarkable interest in many industries. Consequently, the use of numerical calculation methods becomes essential. Lacroix et al. [10] devoted considerable attention to this sort of problem by undertaking a numerical and analytical evaluation of a thermal energy storage system with cylindrical tubes as the energy storage elements. Additionally, Laouadi et al. [11] numerically investigated a system based on the PCM's melting and cyclic solidification. Numerous types of storage units have been designed and studied, as indicated by the preceding studies [3–11]. They all differ in terms of the location of the PCM, the system's configuration, and the type of material used as the storage medium. Currently, the integration of a separate latent storage system is possible either with conventional solar water heaters (that operate via thermosiphon or forced circulation) or with auto-storage collectors [12,13]. However, these approaches are not satisfactory, neither from a thermal perspective (high losses), nor from an aesthetic perspective (tank visible on the outside) [14]. Recent investigations have revealed that the

integration of a thermal storage unit has a considerable impact on the efficiency of the solar collectors [15,16]. Dahou H. et al. [15] experimentally examined the performance of an SWT integrated with nano-enhanced PCM and a Stirrer. The experimental results found that the completion time of the SWT/Ne-PCM system was reduced by 12.5% compared to a conventional tank.

Bouadila S. et al. [16] experimentally examined the performance of a heat pipe-evacuated tube collector integrated with PCM. The experimental results found that the thermal performance of the system was enhanced by adding nanoparticles compared to the conventional case.

To the authors' knowledge, no published study has examined the impact of PCM's thermophysical properties, such as density, enthalpy, and melting temperature, on the load shifting of a solar water heater (SWH) system integrated with PCM. Therefore, the objective of this study is to perform a parametric analysis of the SWH on the basis of PCM's thermophysical properties. Finally, a comparison of SWH–PCM systems with different PCM's thermophysical properties was conducted for introducing the performance of the SWH better, with a series of comparative simulations performed.

2. The Configuration and the Principle of the SWH–PCM System

The configuration of the SWH is shown in Figure 1, which includes a thermal solar collector placed on the roof that captures solar radiation and converts it to thermal energy. A heat transfer fluid (HTF) is heated while passing the solar collector, and flows to a water tank.
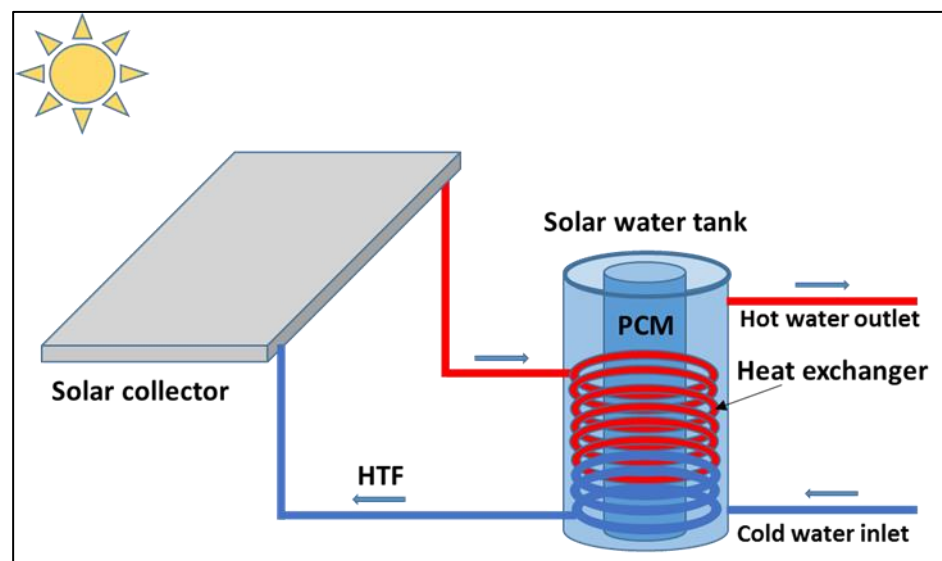

Figure 1. The diagram of the SWH–PCM system.

The computational domain is a water tank configuration such as illustrated in Figure 2, consisting of one inner tube filled with PCM and a spiral heat exchanger tube connected to a solar thermal collector that absorbs and transforms solar energy to thermal energy that is used to heat the HTF passing through the spiral tube. Once the thermal energy absorbed by the HTF is transferred to the water and PCM inside the tank via the spiral tube, the HTF returns to the solar collector to be heated again. The water tank incorporates a heat accumulator, which is comprised of a PCM enclosed in a cylindrical tube. PCM storing and releasing the required thermal energy to maintain the water at hot state. During the daytime while sunlight is available, the water is heated directly by the HTF coming from the solar collector. The available surplus thermal energy is stored in the PCM. When the water tank is refilled at night or when direct solar energy is insufficient, the process is reversed; the PCM releases stored thermal energy, which is transferred to the water. This

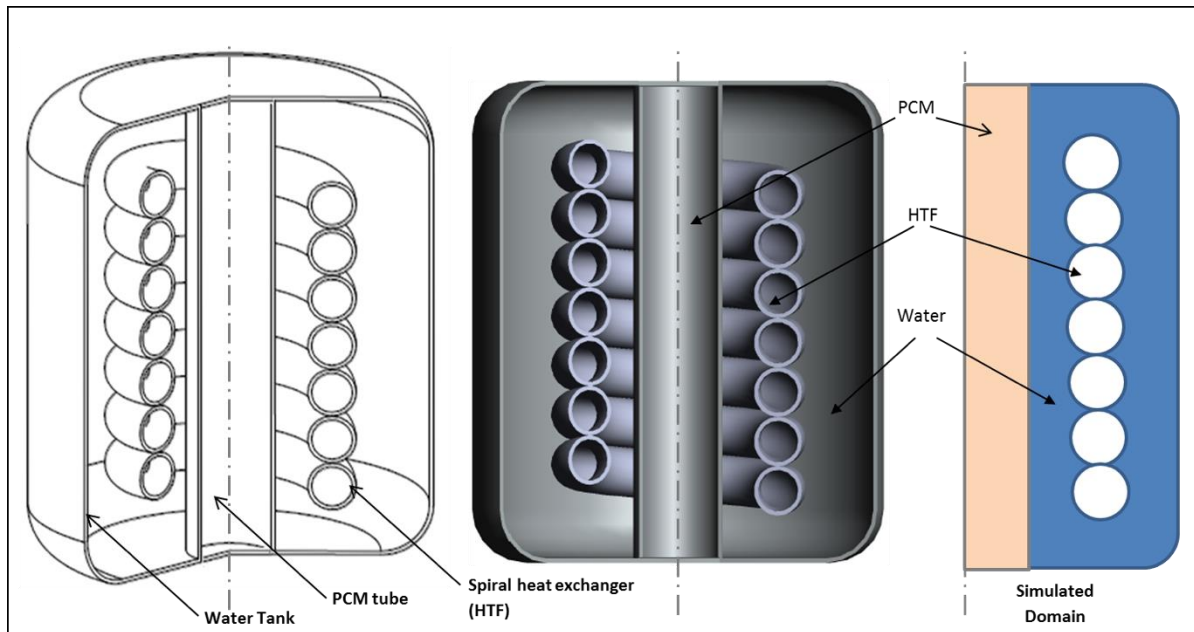design overcomes the intermittent nature of solar energy and keeps the water warm for an extended period.

Figure 2. Numerical modeling and meshing of the studied geometry.

3. Mathematical Model

Based on energy conservation and momentum equations, the mathematical model was developed to predict the thermal behavior and performance of the SWH–PCM system.

The SWH–PCM system is composed of three distinct domains: water, HTF, and PCM. The mathematical model is constructed with the following assumptions:

(i) Constant thermophysical properties [15,16].
(ii) The wall's thermal resistance is negligible [17,18].
(iii) The PCM's volume expansion is negligible [19,20].
(iv) The fluid is assumed to be a Newtonian incompressible fluid [21,22].
(v) The model is simplified to 2D axisymmetric [23,24].

On the basis of the preceding assumptions, the governing equations can be represented as follows:

Continuity equation [25,26]:

$$\frac{\partial \rho}{\partial t} + div\left(\rho \vec{V}\right) = 0 \tag{1}$$

where ρ and $\vec{V}$ denote the liquid's density and velocity, respectively.

Momentum equation [25,26]:

$$\rho \frac{\partial \vec{V}}{\partial t} + \rho \vec{V}.\nabla\left(\vec{V}\right) = -\nabla p + \mu \nabla^2 \vec{V} + \rho \vec{g}\left(T - T_{ref}\right) \tag{2}$$

where p denotes pressure, μ is the liquid's dynamic viscosity, $\vec{g}$ is the gravity vector, and T_{ref} denotes the reference temperature.

Energy equations [25,26]:

For water

$$\rho\, C_P \frac{DT}{Dt} = k\nabla^2 T. \tag{3}$$

where C_P denotes specific heat, k denotes the thermal conductivity, and T denotes temperature.

For PCM

The enthalpy of a material is calculated using the energy equation as the sum of its sensible enthalpy, h, and latent heat, L. The following are the corresponding governing equations [27,28]:

$$\frac{\partial(\rho h)}{\partial t} + \nabla.\left(\rho.\overrightarrow{V}.h\right) = \nabla.(k\nabla T) + S. \tag{4}$$

where h, k, and S denote the enthalpy, the thermal conductivity and the source term, respectively. The following equation expresses the enthalpy, h [27,28]:

$$h = h_{ref} + \int_{T_{ref}}^{T} C_p dT + fL. \tag{5}$$

where h_{ref} and L denote the enthalpy of phase change at the reference temperature T_{ref} and the latent heat of phase change, respectively.

The melted fraction f of PCM is defined as follows [29,30]:

$$f = \begin{cases} 0 & si & T \langle T_{solidus} \\ \frac{T-T_S}{T_S-T_l} & si & T_{solidus} \langle T \langle T_{liquidus} \\ 1 & si & T_{liquidus} \langle T \end{cases} \tag{6}$$

Temperature is essentially a solution obtained by iterating between the energy Equation (4) and the melted fraction Equation (6).

3.1. The Temperature Equation of the HTF

The HTF temperature is considered as variable throughout the day; the variation curve is presented by Salman H. et al. [13]. This curve was fitted and used to determine the HTF temperature equation as a function of time. This equation is a ninth-order polynomial, and its coefficients are listed in Table 1.

$$T_{HTF}(t) = a_0 + a_1 t + a_2 t^2 + \ldots\ldots + a_9 t^9. \tag{7}$$

Table 1. The polynomial coefficients of the HTF temperature equation [13].

a_0	a_1	a_2	a_3	a_4	a_5	a_6	a_7	a_8	a_9
281.316	0.0025	-3.881×10^{-7}	4.601×10^{-11}	-1.907×10^{-15}	3.050×10^{-20}	-3.307×10^{-26}	-4.699×10^{-30}	5.27×10^{-35}	-1.814×10^{-40}

3.2. The Storage Efficiency of the SWH–PCM System

In order to analyze the heat storage efficiency of the SWH–PCM system, the heat storage efficiency was calculated by following equation [31,32]:

$$\eta_{SWH} = \frac{Q_{re}}{Q_{st}}. \tag{8}$$

where the Q_{re} and Q_{st} are the total released thermal energy and stored thermal energy, respectively.

The stored thermal energy of the SWH–PCM system is given by:

$$Q_{st} = m\int_{T_0}^{T_m} C_{p,s} dT + mf\Delta H + m\int_{T_m}^{T_a} C_{p,l} dT. \tag{9}$$

The released thermal energy of the SWH–PCM system is given by

$$Q_{re} = m \int_{T_0}^{T_m} C_{p,liq} dT + mf\Delta H + m \int_{T_m}^{T_a} C_{p,solid} dT \tag{10}$$

where m is the mass of PCM, T_0 is the initial temperature of the PCM, T_m is the melting temperature, and T_a is the average temperature of PCM at the end of the melting process

3.3. Boundary Conditions

The configuration of the SWH–PCM system illustrated in Figure 2 was created using Gambit software, considering the following initial and boundary conditions [33,34]:
(i) Initially, it is assumed that the temperatures of PCM, HTF, and water are uniform;
(ii) External wall of the SWH–PCM system is thermally insulated;
(iii) The temperature of the HTF is variable with time as expected in Equation (7);
(iv) The interface between the domains is considered thermally coupled [35].

4. Simulation Method and Model Validation

The physical model was simulated numerically using the Ansys. 14, which employs the finite volume method. The software was used to mesh the SWH–PCM system configuration, which has 3500 triangular meshes. The mesh's influence on the simulation was tested (a model with a maximum of 5000 meshes was tested). The presented results are independent of the mesh as of the computation time step (time steps varying between 0.01 and 30 s). The flowchart in Figure 3 depicts the overall procedure for simulating the studied system.
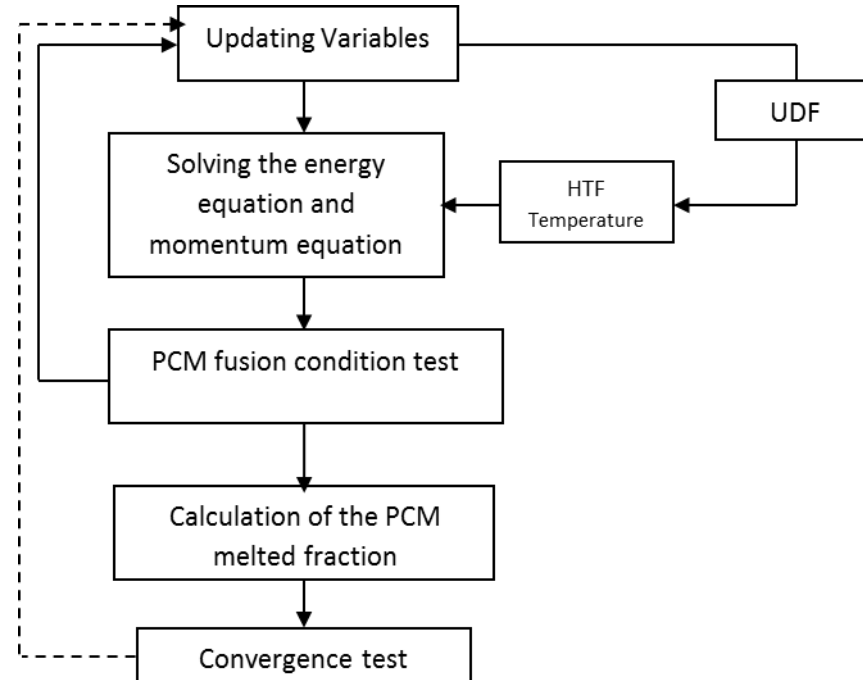

Figure 3. Flowchart showing steps of calculation algorithm.

Under the same operation conditions and geometric parameters, the numerical prediction of the physical model was compared with that in the literature results [14]. Figure 4 illustrates the comparative results, which demonstrate a high degree of consistency between the simulation data and the reference data. As a result, the physical model was deemed acceptable and reliable.
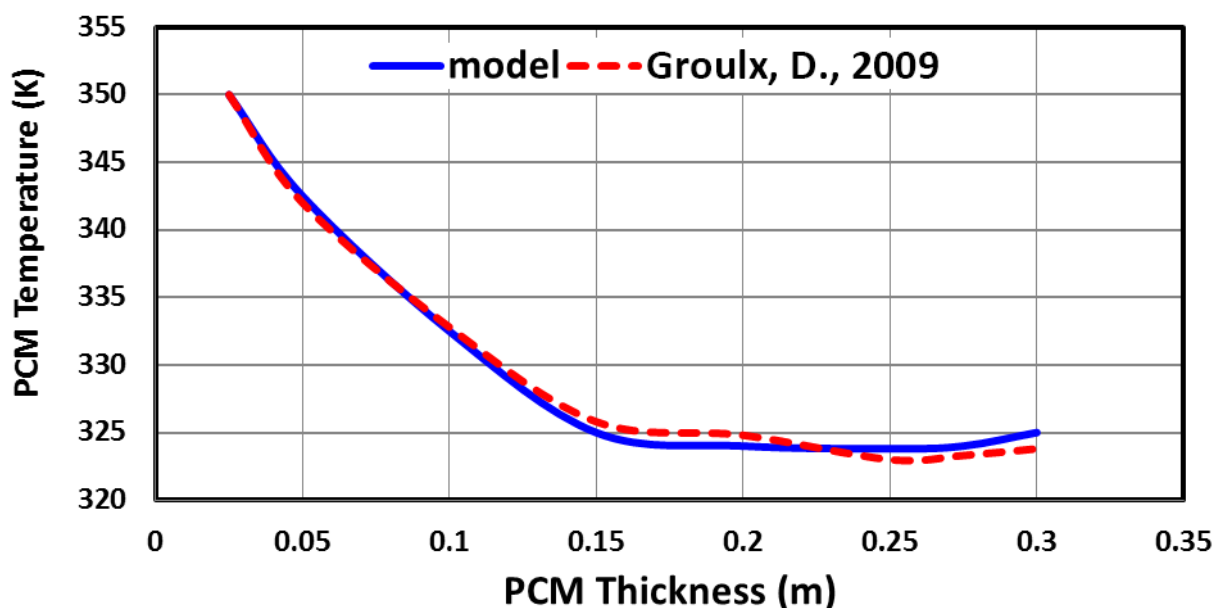
Figure 4. Validation of the mathematical model [14].

5. Results and Discussion

The numerical analysis was performed on a cylindrical water tank with a diameter of 0.30 m and a height of 0.60 m, which comprised a cylinder with a diameter of 0.10 m filled with paraffin wax (melting range: 50–52 °C). Additionally, the water tank incorporates a spiral heat exchanger that circulates heated HTF to pass through (it reaches a maximum value 87 °C greater than the PCM melting temperature). Table 2 shows the thermo-physical proprieties of the PCM.

Table 2. The PCM's thermo-physical properties.

Melting point	50 °C
Latent heat	145 KJ/kg
Viscosity	1.9 mm^2
Density	1412 kg/m^3
Specific heat	2.4 KJ/kgK
Thermal conductivity	0.2 W/mK

Figures 5 and 6 depict, respectively, the temperature distribution of the SWH–PCM and the melted fraction of the PCM at selected times during the charging/discharging cycle. In the initial phase of the charging procedure, the temperature of the PCM (Figure 5) at the interface with the water tank begins to rise, and the PCM then begins to transform into a liquid state (Figure 6). Once the water temperature approaches the saturation point at 13:30 (Figure 5), just a small percentage of PCM remains unmelted (Figure 6). This demonstrates that the PCM quantity is sufficient to preserve all the excess heat absorbed over the day.

During the night, beginning at 18:00, the PCM begins to solidify and release its stored heat (Figure 6), causing the water temperature in the tank to increase (Figure 5).

The average water temperature evolution in the SWH system with and without PCM during a charging/discharging cycle is depicted in Figure 7. Initially, it was observed that the two cases exhibit identical curve shapes. Nonetheless, commencing around 11:30, a load shift was noted between the two profiles. The difference in water temperature between the two cases is related to the amount of heat stored in the PCM. In addition, a second load shift was observed during the discharge process between 19:00 and 22:00. As can be

observed, the average water temperature difference between the two cases might approach 9 degrees.
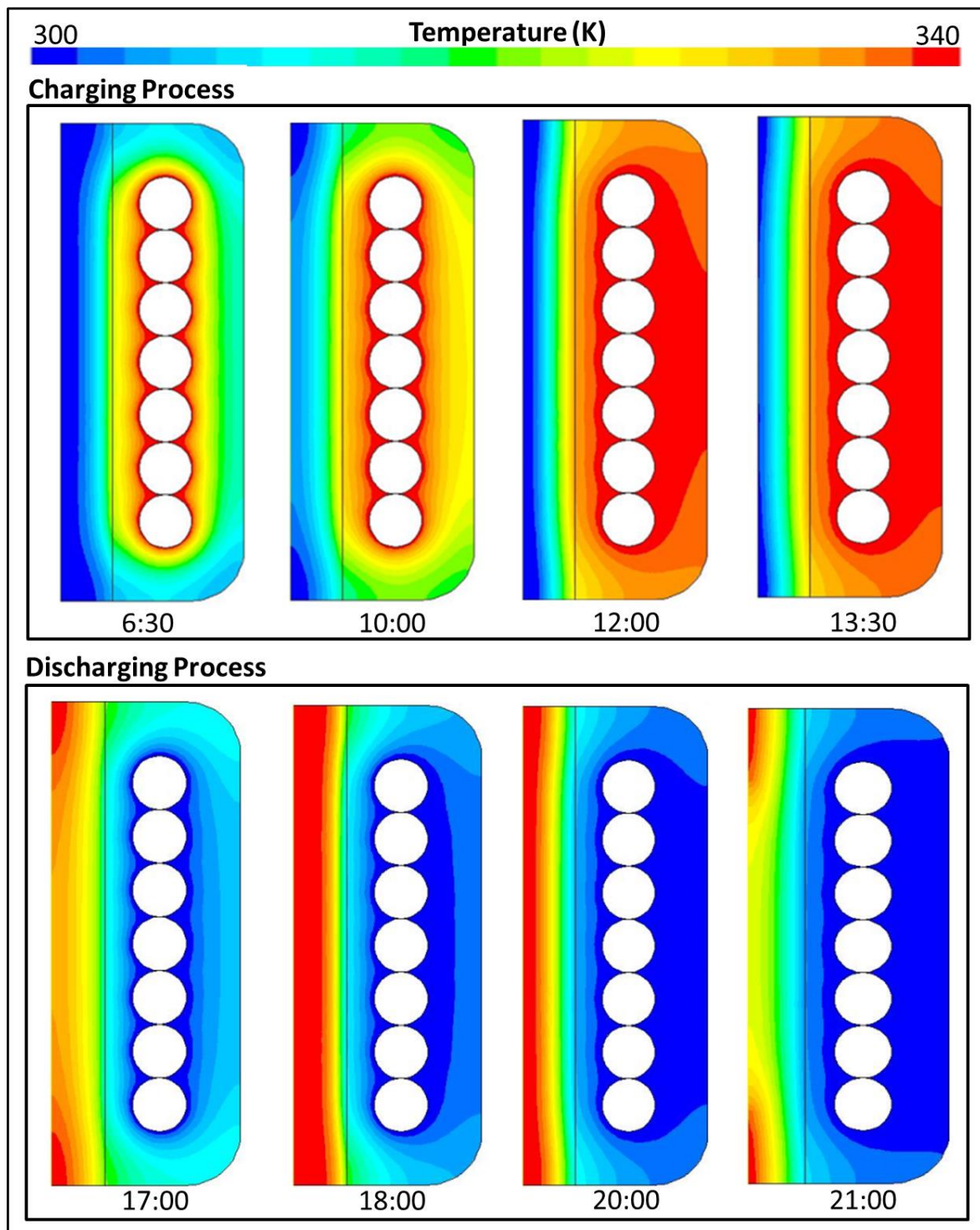

Figure 5. Time distribution of the temperature of the SWH–PCM system at selected times.
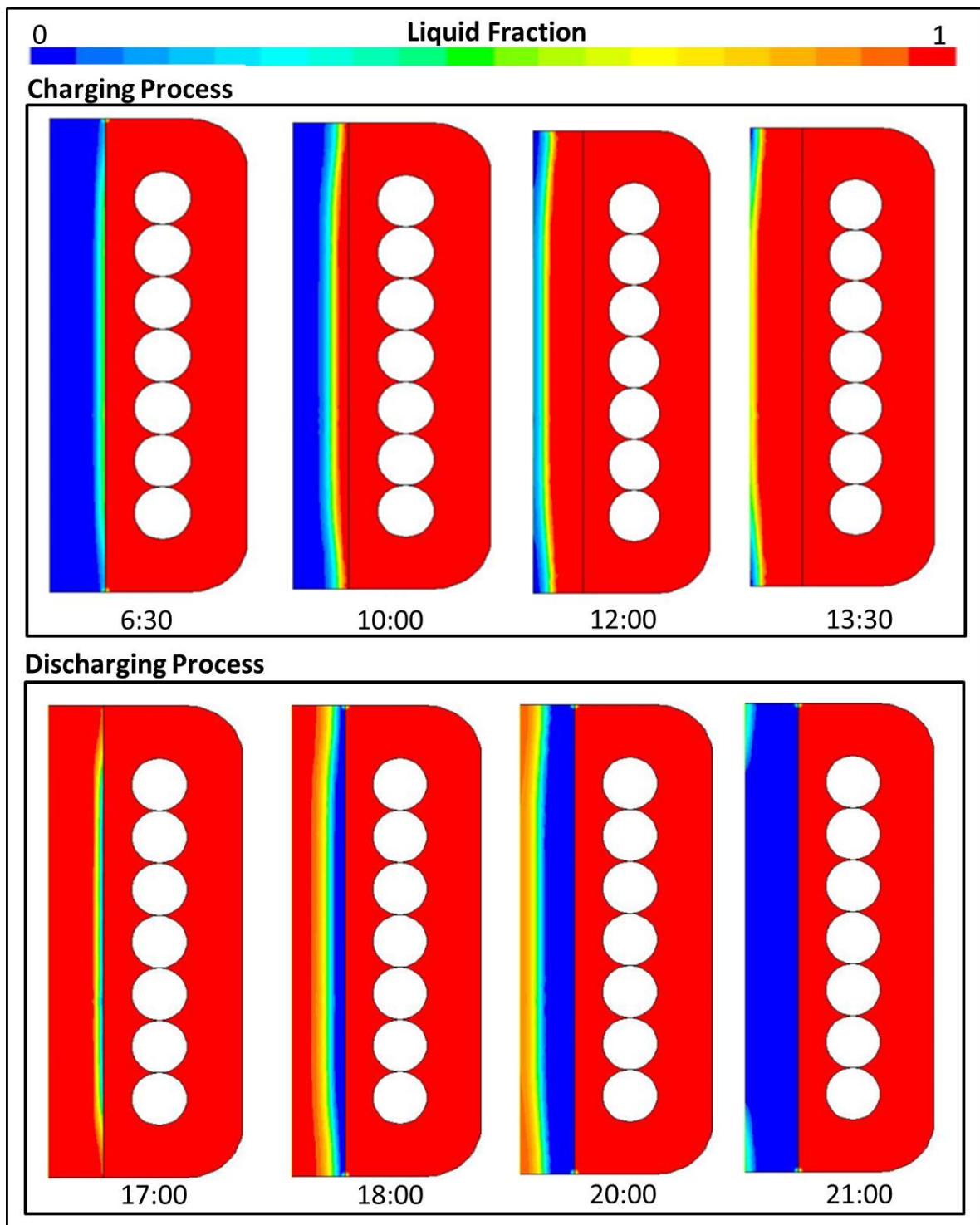
Figure 6. Time distribution of the melted fraction of the PCM at selected times.
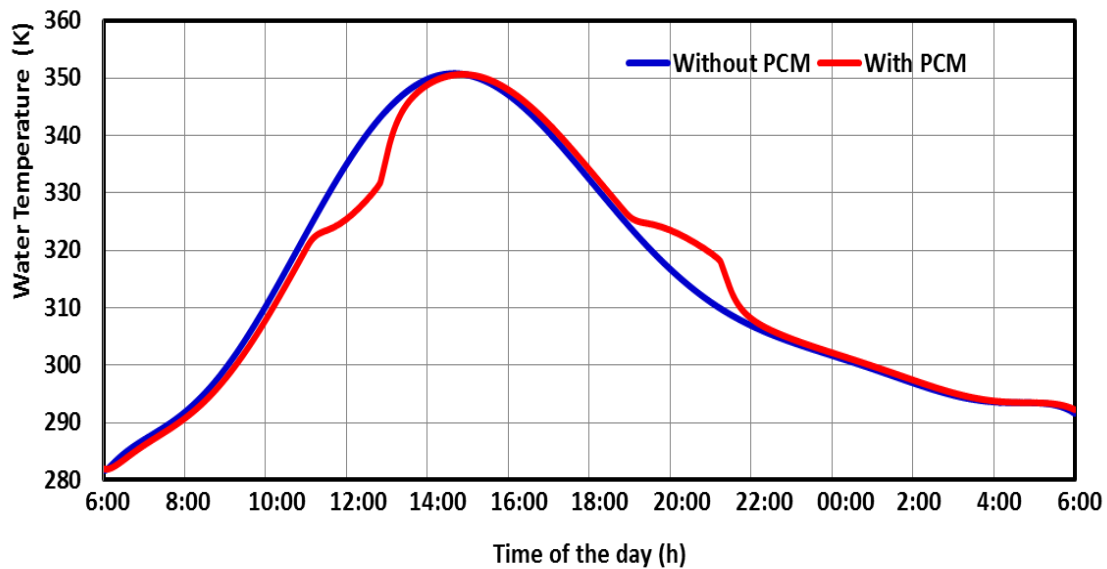
Figure 7. Time evolution of average water temperature for the cases with PCM and without PCM during a complete cycle (charging/discharging).

The melted fraction of the PCM evolution is depicted in Figure 8. The curve can be divided into three parts: the first, in which the PCM stores energy through sensible heat; the second, in which the temperature remains constant during phase change and the PCM stores a large amount of heat due to its latent heat; and the third, which is similar to the first, except the PCM is completely liquid. Observably, the melted fraction remains constant between 6:00 and 11:00, indicating that the PCM's temperature is below its melting point and that the storage is sensible. During the periods of 11:00 to 13:00, the temperature of the tank reaches the PCM's melting point, causing the melted fraction to rapidly increase to one, indicating that the PCM has entirely melted. After 13:00, the melted fraction remains constant until 19:00 (sensible storage) due to the tiny temperature differential between the tank and PCM. Then, as the water temperature falls below the melting point of the PCM, the solidification process begins, and the melted fraction rapidly decreases until it reaches zero (the PCM becomes solid again). Finally, between 21:25 and 6:00, the melted fraction remains constant, indicating that thermal equilibrium has been reached.
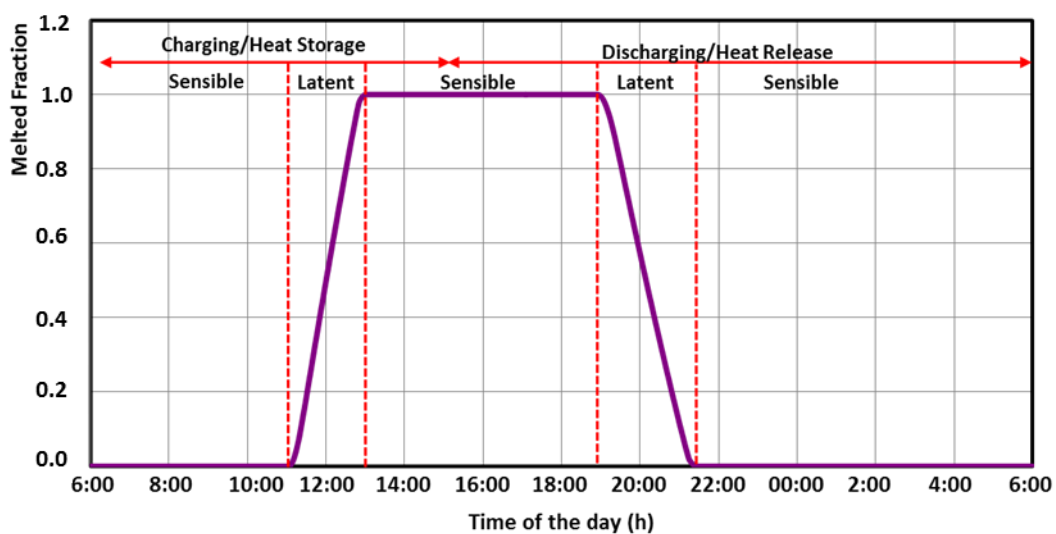

Figure 8. Time evolution of average melted fraction of the PCM during a complete cycle (charging/discharging).

The effect of PCM density on the rate of heat transfer to/from PCM and the PCM melted fraction is depicted in Figure 9. Four cases were analyzed with different densities of PCM (1412, 2000, 2824, and 3200 kg/m^3). Figure 9a depicts the variations of the heat flux transferred to/from PCM, while Figure 9b depicts the time-dependent evolution of the melted fraction. As shown in Figure 9a, the quantity of heat stored by the PCM is proportional to its density. It is evident that an increase in density increases the quantity of energy stored. This increase in stored energy slows down the fusion process of the PCM, resulting in a greater load shift, as shown in Figure 9b.
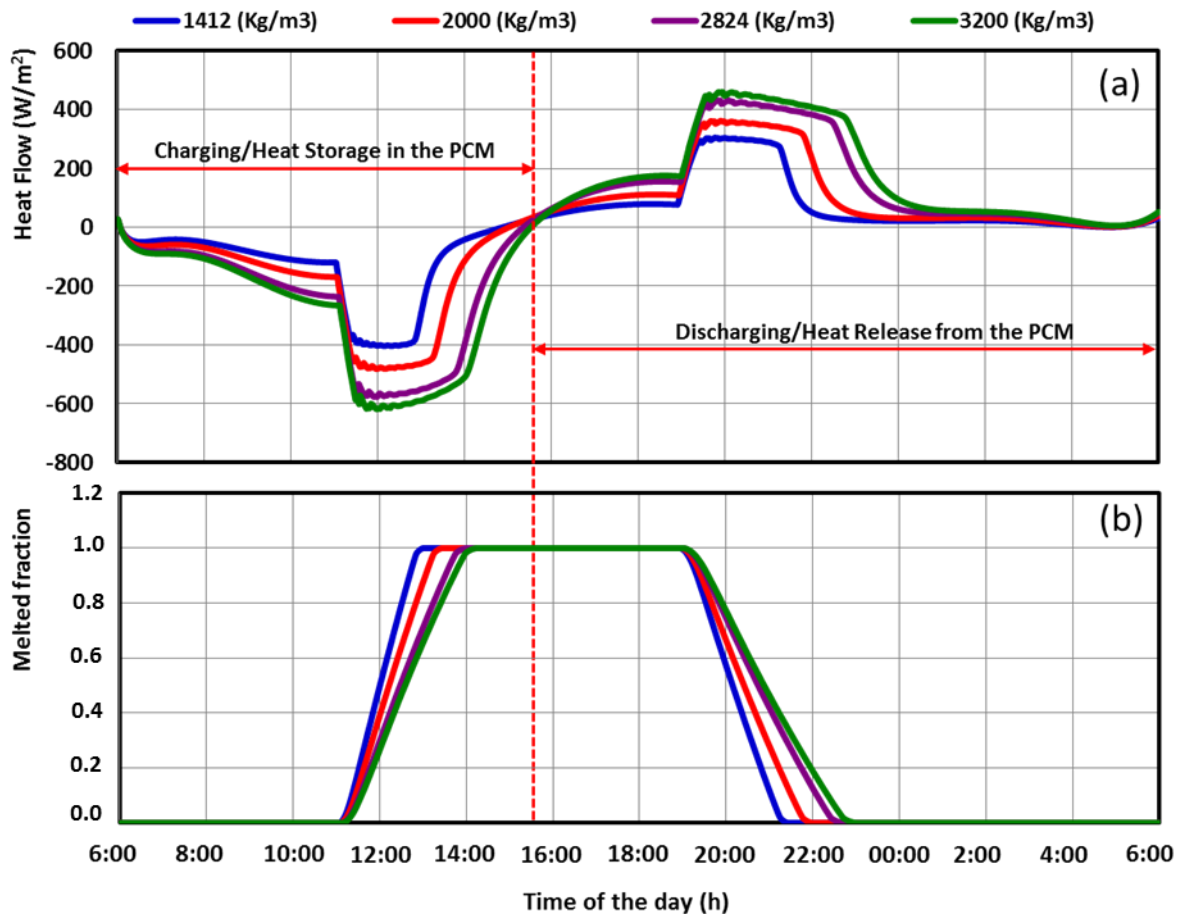

Figure 9. The effect of the PCM density on: (**a**) the average heat flow transferred to/from PCM; and (**b**) the average PCM melted fraction.

Figure 10 depicts the effect of PCM enthalpy on the average water temperature and the PCM melted fraction. Six cases were analyzed with different enthalpies of PCM (0, 100, 145, 235, 520, and 190 kJ/kg). Figure 10a shows the changes in water temperature, whereas Figure 10b shows the time-dependent evolution of the melted fraction. As depicted in Figure 10a, raising the PCM enthalpy slows the increase in water temperature in the morning and the reduction in water temperature at night. This is due to the fact that when the PCM's enthalpy is high, it holds more heat, resulting in less heat transfer to the water. This reduction in heat transfer reduces the PCM fusion process rate, resulting in a greater load shift, as shown in Figure 10b.
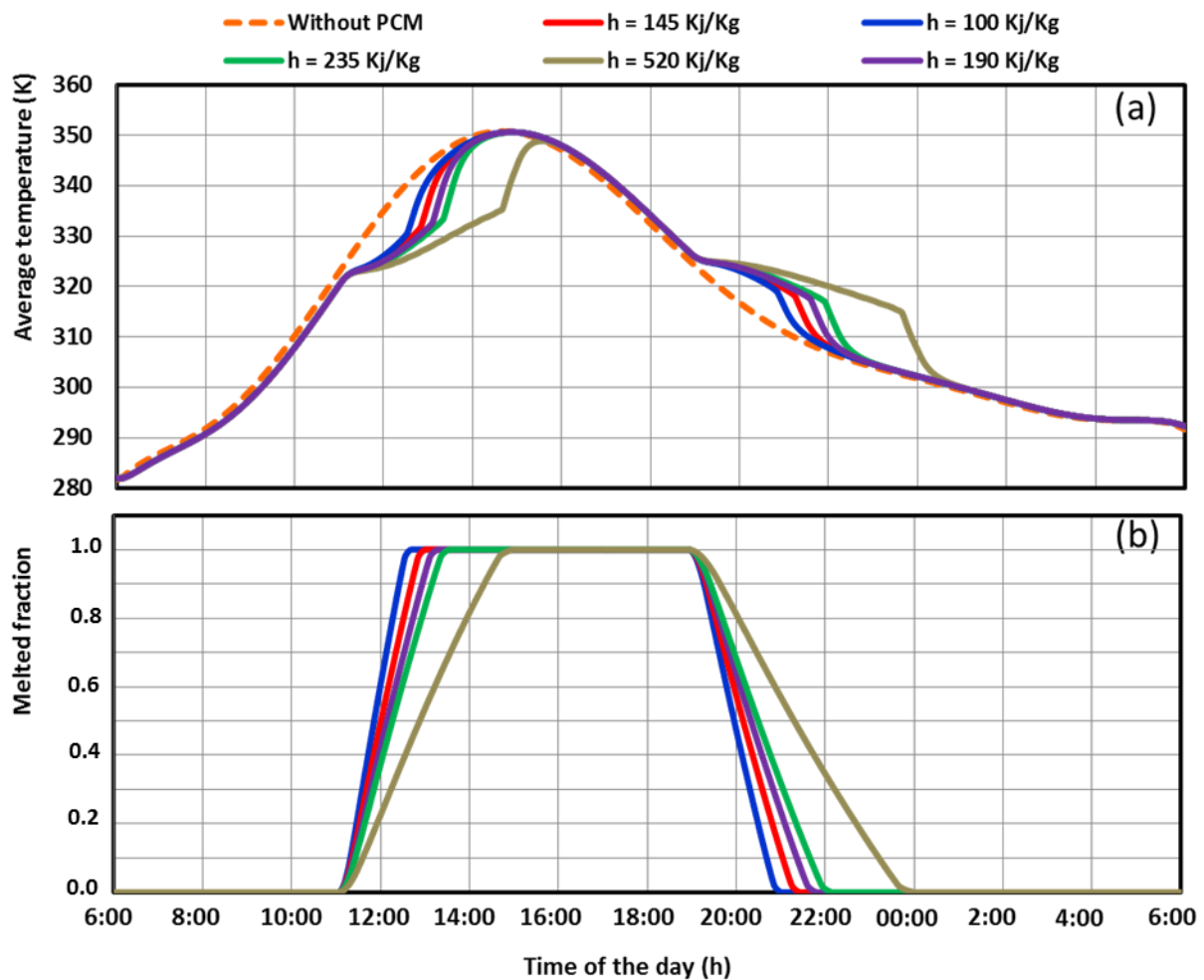
Figure 10. The effect of the PCM enthalpy on: (**a**) the average water temperature; and (**b**) the average PCM melted fraction.

The effect of the PCM melting temperature on the rate of heat transfer to/from PCM and the PCM melted fraction is depicted in Figure 11. Four cases were analyzed with different melting temperature of PCM (313, 323, 333, and 343 K). Figure 11a depicts the variations of the heat flux transferred to/from PCM, while Figure 11b depicts the time-dependent evolution of the melted fraction. As shown in Figure 11a, the duration of the fusion process of the PCM is related to the PCM melting temperature. It is evident that a decrease in the PCM melting temperature increases the duration of the fusion process of the PCM. This increase in duration of the fusion process of the PCM increases the possibility of having warm water late at night, as shown in Figure 11b. For instance, PCM with a melting temperature of 343 K begins solidifying as soon as it becomes completely molten, but PCM with a melting temperature of 313 K takes a lengthy time to begin solidifying (more than 8 h). Therefore, a lower melting temperature is preferred when a longer fusion process duration is desired.
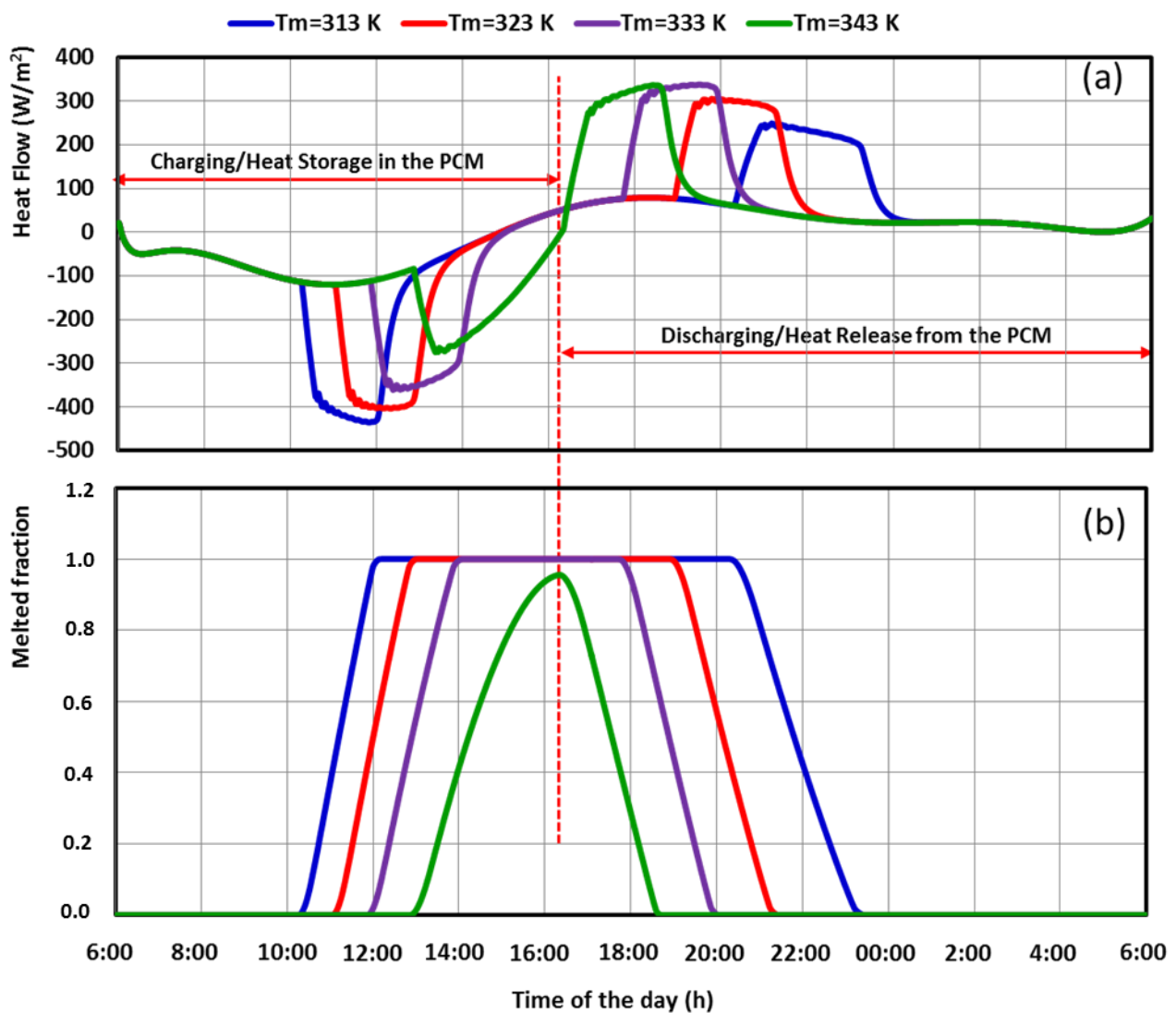
Figure 11. The effect of the PCM melting temperature on: (**a**) the average heat flow transferred to/from PCM; and (**b**) the average PCM melted fraction.

The literature shows a limited number of investigations on PCM thermal storage tanks coupled with a solar thermal collector to provide domestic hot water. To assess the effectiveness of various TES with PCMs for SWHs proposals, several experimental and numerical studies have been developed. The majority of this research asserted that it showed the beneficial effects of adding PCMs in terms of various methods and criteria, including system efficiency, energy storage capacity, shifting hours, and energy savings. In order to present the practicality of the proposed system and its efficiency in comparison with other proposed systems, the maximum outlet water temperature and the highest thermal efficiency obtained from the proposed system were compared to that obtained by the previous studies [27,36,37] and presented in Table 3.

A. Bayomy et al. [36] developed a solar system that utilizes an n-eicosane PCM as the thermal store medium in domestic hot water. The results revealed that the system can reach an efficiency of 39%. Kılıçkap S. et al. [27] investigated an SWH tank utilizing a thermal energy storage (TES) tank. In their research, it was found that the SWH–PCM tank has an efficiency of 58%. Harris B. et al. [37] implemented a redesign methodology to enhance an existing TES with PCM system for a SWH tank. Their results show that the redesigned TES reached a minimum outlet water temperature of 45.30 °C and a thermal efficiency of 76.08%. However, in the present study, a water tank with latent heat storage

in combination with a hot water collector was tested, and the highest thermal efficiency value in the study was obtained as 76.3%. Table 3 shows the present SWH–PCM system accomplished the best performance compared to the previous studies. It reaches higher outlet water temperatures during charging and higher thermal efficiency. Table 3 shows that the maximum outlet water temperature in the present study was always higher than that obtained by ref. [27,36,37]. This can be explained by the using of the higher melting temperature PCM (50 °C) compared to the previous studies.

Table 3. Comparison of key performance indicators related to the present SSWH–PCM system and that for the previous studies.

Parameters	Ref. [36]	Ref. [27]	Ref. [37]	Present Study
PCM melting temperature	36.4 °C	35 °C	43.9 °C	50 °C
Maximum outlet water temperature	52 °C	73 °C	51.3 °C	77 °C
Highest thermal efficiency (SSWH–PCM system)	39%	54%	76.08%	76.3%

As was demonstrated, using PCMs rather than traditional water storage might make sense in order to increase the solar system's autonomy. However, care should be used when selecting PCM. The melting range of the fitted PCM should be comparable to the temperatures attained in the storage tank. Higher storage tank temperatures result in a rapid decline in PCM's heat capacity and increased water efficiency. From this comparison, it was also demonstrated that lower PCM melting temperature is not effective for the system, especially in summer, when sun irradiation is greater and tank temperatures are correspondingly much higher.

6. Conclusions

In this study, a number of numerical simulations were conducted to examine the impact of modifying the thermo-physical proprieties of the PCM that is integrated with the SWH system. A two-dimensional mathematical model was developed to predict the dynamic behavior of the SWH–PCM system. Using this model, numerous numerical simulations were conducted, and the following findings were obtained:

- The highest thermal efficiency of the new SWH–PCM system is 76.3%.
- There is an optimal latent heat for which the heat storage system is optimized in terms of heat stored and energy recovery efficiency of the SWH–PCM system. This optimal latent heat value is around 520 kj/kg.
- For the new SWH–PCM system, compared with SWH integrated with PCM density of 1412 kg/m^3, the effective heat collection time is prolonged up to 21.1 % for the case with PCM density of 3200 kg/m^3.
- Utilization of PCM with lower melting temperature is beneficial to enhance energy performance of an SWH. The optimal T_m value is around 313 K which gives maximum energy recovery efficiency of 32.1%.
- The integration of PCM with SWH can shift 20,2 % of peak thermal energy load to off-peak periods.
- Load shifting can be increased by increasing density and latent heat of PCM.
- The water temperature can be maintained at a greater degree throughout the night for a longer period of time when using a PCM with lower melting temperature.

Author Contributions: Conceptualization, S.M. and T.A.; methodology, S.A.; software, S.M.; validation, S.M., T.A. and S.A.; formal analysis, T.A.; investigation, S.M.; resources, T.A.; data curation, T.A.; writing—original draft preparation, S.M.; writing—review and editing, T.A.; visualization, S.A.; supervision, S.M.; project administration, S.M.; funding acquisition, S.A. All authors have read and agreed to the published version of the manuscript.

Conflicts of Interest: The authors declare no conflict of interest.

Nomenclature

C_P	specific heat (kj/kg·K)
F	the melted fraction of PCM
$\vec{g}$	the acceleration of gravity (m/s^2)
h	the enthalpy (kj/kg)
k	the thermal conductivity (W/m·K)
L	the latent heat (kj/kg)
P	pressure (Pa)
S	the source term (kj/kg)
T	the temperature (K)
$\vec{V}$	the velocity (m/s)
ρ	the liquid's density (kg/m^3)
μ	the liquid's dynamic viscosity (Pa s)

Subscript

ref	the reference

Abbreviations

HTF	Heat Transfer Fluid
PCM	Phase Change Material
SWH	Solar Water Heater

References

1. Elarem, R.; Alqahtani, T.; Mellouli, S.; Askri, F.; Edacherian, A.; Vineet, T.; Badruddin, I.A.; Abdelmajid, J. A comprehensive review of heat transfer intensification methods for latent heat storage units. *Energy Storage* **2021**, *3*, e1272021. [CrossRef]
2. Khan, M.M.A.; Ibrahim, N.I.; Mahbubul, I.M.; Ali, H.M.; Saidur, R.; Al-Sulaiman, F.A. Evaluation of solar collector designs with integrated latent heat thermal energy storage: A review. *Sol. Energy* **2018**, *166*, 334–350. [CrossRef]
3. Sharma, A.; Tyagi, V.V.; Chen, C.R.; Buddhi, D. Review on thermal energy storage with phase change materials and applications. *Renew. Sustain. Energy Rev.* **2009**, *13*, 318–345. [CrossRef]
4. Kurklu, A.; Ozmerzi, A.; Bilgin, S. Thermal Performance of a Water-Phase ChangeMaterial Solar Collector. *Renew. Energy* **2002**, *26*, 391–399. [CrossRef]
5. Zalba, B.; Marín, J.M.; Cabeza, L.F.; Mehling, H. Review on thermal energy storage with phase change: Materials, heat transfer analysis and applications. *Appl. Therm. Eng.* **2003**, *23*, 251–283. [CrossRef]
6. Eames, P.; Griffiths, P. Thermal behaviour of integrated solar collector/storage unit with 65 °C phase change material. *Energy Convers. Manag.* **2006**, *47*, 3611–3618. [CrossRef]
7. Plantier, C. Etude Numérique et Expérimentale d'un Prototype de Chauffe-eau Solaire Équipé d'un Stockage à Chaleur Latente. Ph.D. Thesis, ESIGEC—Univérsité de Savoie, Chambéry, France, 2005.
8. Haillot, D.; Goetz, V.; Py, X.; Abdelkarim, M.B. Integrated solar collector storage system based on phase change material and graphite composite. In Proceedings of the EUROSUN 2008, 1st International Congress on Heating, Cooling and Buildings, Lisbon, Portugal, 7–10 October 2008.
9. Mettaweea, E.B.S.; Assassab, G.M.R. Experimental Study of a Compact PCM Solar Collector. *Energy* **2006**, *31*, 2958–2968. [CrossRef]
10. Lacroix, M. Study of the Heat Transfer Behavior of Latent Heat Thermal Energy StorageUnit with a Finned Tube. *Int. J. Heat Mass Transf.* **1993**, *36*, 2083–2092. [CrossRef]
11. Laouadi, A.; Lacroix, M. Thermal performance of a latent heat energy storage ventilated panel for electric load management. *Int. J. Heat Mass Transf.* **1999**, *42*, 275–286. [CrossRef]
12. Farid, M.M.; Husian, R.M. An electrical storage heater using the phase-change method of heat storage. *Energy Convers. Manag.* **1990**, *3*, 219–230. [CrossRef]
13. Hammadi, S.H. Study of solar water heating system with natural circulation in basrah. *Al-Qadisiya J. Eng. Sci.* **2009**, *2*.
14. Groulx, D.; Ogoh, W. Solid-Liquid Phase Change Simulation Applied to a Cylindrical Latent Heat Energy Storage System. In Proceedings of the COMSOL Conference 2009, Boston, MA, USA, 8–10 October 2009.

15. Dhaou, M.H.; Mellouli, S.; Alresheedi, F.; El-Ghoul, Y. Experimental assessment of a solar water tank integrated with nano-enhanced PCM and a stirrer. *Alex. Eng. J.* **2022**, *61*, 8113–8122. [CrossRef]

16. Bouadila, S.; Baddadi, S.; Rehman, T.-U.; Ayed, R. Experimental investigation on the thermal appraisal of heat pipe-evacuated tube collector-based water heating system integrated with PCM. *Renew. Energy* **2022**, *199*, 382–394. [CrossRef]

17. Paing, S.T.; Anderson, T.N.; Nates, R.J. Reducing heat loss from solar hot water storage tanks using passive baffles. *J. Energy Storage* **2022**, *52*, 104807. [CrossRef]

18. Pathak, S.K.; Tyagi, V.V.; Chopra, K.; Sharma, R.K. Recent development in thermal performance of solar water heating (SWH) systems. *Mater. Today Proc.* **2022**, *63*, 778–785. [CrossRef]

19. Ahmed, S.F.; Khalid, M.; Vaka, M.; Walvekar, R.; Numan, A.; Rasheed, A.K.; Mubarak, N.M. Recent progress in solar water heaters and solar collectors: A comprehensive review. *Therm. Sci. Eng. Prog.* **2021**, *25*, 100981. [CrossRef]

20. Algarni, S.; Mellouli, S.; Alqahtani, T.; Almutairi, K.; Khan, A.; Anqi, A. Experimental investigation of an evacuated tube solar collector incorporating nano-enhanced PCM as a thermal booster. *Appl. Therm. Eng.* **2020**, *180*, 115831. [CrossRef]

21. Xue, H.S. Experimental investigation of a domestic solar water heater with solar collector coupled phase-change energy storage. *Renew. Energy* **2016**, *86*, 257–261. [CrossRef]

22. Saraswat, A.; Bhattacharjee, R.; Verma, A.; Das, M.K.; Khandekar, S. Investigation of diffusional transport of heat and its enhancement in phase-change thermal energy storage systems. *Appl. Therm. Eng.* **2017**, *111*, 1611–1621. [CrossRef]

23. Papadimitratos, A.; Sobhansarbandi, S.; Pozdin, V.; Zakhidov, A.; Hassanipour, F. Evacuated tube solar collectors integrated with phase change materials. *Sol. Energy* **2016**, *129*, 10–19. [CrossRef]

24. Eslamnezhad, H.; Rahimi, A. Enhance heat transfer for phase-change materials in triplex tube heat exchanger with selected arrangements of fins. *Appl. Therm. Eng.* **2017**, *113*, 813–821. [CrossRef]

25. Seddegh, S.; Wang, X.; Henderson, A.D.; Xing, Z. Solar domestic hot water systems using latent heat energy storage medium: A review. *Renew. Sustain. Energy Rev.* **2015**, *49*, 517–533. [CrossRef]

26. Fazilati, M.; Alemrajabi, A.A. Phase change material for enhancing solar water heater, an experimental approach. *Energy Convers. Manag.* **2013**, *71*, 138–145. [CrossRef]

27. Kılıçkap, S.; El, C.; Yıldız, E. Investigation of the effect on the efficiency of phase change material placed in solar collector tank. *Therm. Sci. Eng. Prog.* **2018**, *5*, 25–31. [CrossRef]

28. Pandey, A.; Hossain, M.; Tyagi, V.; Rahim, N.A.; Selvaraj, J.A.; Sari, A. Novel approaches and recent developments on potential applications of phase change materials in solar energy. *Renew. Sustain. Energy Rev.* **2018**, *82*, 281–323. [CrossRef]

29. Al-Kayiem, H.H.; Lin, S.C. Performance evaluation of a solar water heater integrated with a PCM nanocomposite TES at various inclinations. *Sol. Energy* **2014**, *109*, 82–92. [CrossRef]

30. Chaabane, M.; Mhiri, H.; Bournot, P. Thermal performance of an integrated collector storage solar water heater (ICSSWH) with phase change materials (PCM). *Energy Convers. Manag.* **2014**, *78*, 897–903. [CrossRef]

31. Abokersh, M.H.; El-Morsi, M.; Sharaf, O.; Abdelrahman, W. On-demand operation of a compact solar water heater based on U-pipe evacuated tube solar collector combined with phase change material. *Sol. Energy* **2017**, *155*, 1130–1147. [CrossRef]

32. Swiatek, M.; Fraisse, G.; Pailha, M. Stratification enhancement for an integrated collector storage solar water heater (ICSSWH). *Energy Build.* **2015**, *106*, 35–43. [CrossRef]

33. Mahfuz, M.; Anisur, M.; Kibria, M.; Saidur, R.; Metselaar, I. Performance investigation of thermal energy storage system with Phase Change Material (PCM) for solar water heating application. *Int. Commun. Heat Mass Transf.* **2014**, *57*, 132–139. [CrossRef]

34. Mazman, M.; Cabeza, L.F.; Mehling, H.; Nogues, M.; Evliya, H.; Paksoy, H. Utilization of phase change materials in solar domestic hot water systems. *Renew. Energy* **2009**, *34*, 1639–1643. [CrossRef]

35. Mohamed, S.A.; Al-Sulaiman, F.A.; Ibrahim, N.I.; Zahir, H.; Al-Ahmed, A.; Saidur, R.; Yılbaş, B.S.; Sahin, A.Z. A review on current status and challenges of inorganic phase change materials for thermal energy storage systems. *Renew. Sustain. Energy Rev.* **2017**, *70*, 1072–1089. [CrossRef]

36. Ayman, B.; Stephen, D.; Ziad, S. Domestic Hot Water Storage Tank Utilizing Phase Change Materials (PCMs): Numerical Approach. *Energies* **2019**, *12*, 2170. [CrossRef]

37. Harris Bernal, I.A.; James Rivas, A.M.; Ortega Del Rosario, M.D.L.A.; Saghir, M.Z. A Redesign Methodology to Improve the Performance of a Thermal Energy Storage with Phase Change Materials: A Numerical Approach. *Energies* **2022**, *15*, 960. [CrossRef]